

3D SHAPE OPTIMISATION OF TURBOMACHINERY BLADING

PIOTR LAMPART¹ AND SERGEY YERSHOV²

¹*Institute of Fluid Flow Machinery,
Polish Academy of Sciences,
Fiszera 14, 80-952 Gdansk, Poland
lampart@imp.gda.pl*

²*Institute of Mechanical Engineering Problems,
Ukrainian National Academy of Sciences,
2/10 Pozharsky, 310046 Kharkov, Ukraine
yershov@online.kharkiv.com*

(Received 30 August 2001)

Abstract: The shape of HP gas and steam turbine stages, as well as of an LP exit stage of a steam turbine, is optimised numerically using a code *Optimus* and 3D RANS solver *FlowER*. The numerical method draws on direct constrained optimisation based on the method of deformed polyhedron. Values of the minimised objective function, that is stage losses with the exit energy are found from 3D viscous compressible computations. There are constraints imposed on the mass flow rate, exit swirl angle and reactions. Among the optimised parameters are stator and rotor blade numbers, stagger and twist angles, stator sweep and lean, both straight and compound. The optimisation gives new 3D designs with increased efficiencies.

Keywords: turbomachinery blading, blade shape optimisation, CFD

1. Introduction

The efficiency of turbine stages can be increased by optimisation of 3D blading. Due to many ways of 3D blade stacking (only to mention lean, sweep, twist – straight or compound, or combinations of the above) and a large number of shape parameters that can effect flow patterns and efficiencies, it is highly required that automatic optimisation techniques and automatic changing of flow geometry corresponding to the shape parameters obtained in the process of optimisation are used so as to find the optimum design.

Therefore, works on optimisation of turbomachinery blading based on 3D codes are in progress. Results of 3D inverse design using Euler or Navier-Stokes codes are reported by Demeulenaere and Van Den Braembussche [1], Damle *et al.* [2]. A concept of 2D/3D optimisation with the help of an artificial neural network trained over a data base of RANS solutions is presented by Pierret and Van Den Braembussche [3], Pierret [4]. A brief literature review of shape optimisation of turbomachinery blades and

aerodynamic shapes, as well as a comparative study of optimisation methods including genetic algorithms, simulated annealing and sequential quadratic programming, can be found in a paper of Shahpar [5].

This paper pursues the idea of direct optimisation where the final shape of the blading is obtained from minimising/maximising an objective function, for example the total energy loss or efficiency, total pressure loss of the stage *etc.*, and where the current values of the objective function are found from 3D RANS computations of geometries changed during the process of optimisation. An example of direct efficiency-based optimisation of the 3D stacking lines for compressor blading without changing the blade section can be found in Lee and Kim [6]. In the present paper, efforts are also concentrated on optimising the 3D stacking line for the stator blade, trying the use of stator and rotor blade twist as well as stator blade lean and sweep, while keeping the blade section unchanged. The optimisation is carried out using Nelder-Mead's method of deformed polyhedron, which is relatively easy to work with constraints imposed on the mass flow rate, reaction and exit angle.

Major effects of 3D blade stacking are known, see Harrison [7], Denton and Xu [8], Singh et al. [9], Wang [10], Lampart and Gardzilewicz [11]. 3D blade stacking redistributes blade load, mass flow rate and loss span-wise, compared to the cylindrical blading. The sole fact of using 3D stacking lines for turbine blading does not necessarily mean largely increased efficiencies. The quantitative effect of 3D blade stacking on the overall loss coefficient of the turbine stage depends on the method of stacking and varies with stage geometry, especially with the span/chord ratio. No matter how large are efficiency gains from 3D blade stacking, the optimisation of turbine stages based on 3D solvers may also help in what was earlier a domain of classical 1D optimisation, that is optimisation of pitch/chord and span/chord ratios and stagger angles. This is due to a simple fact that the flow past the cylindrical turbine blading is already fully 3D.

2. Optimiser

Mathematically, the process of optimisation is an iterative procedure that seeks for an extremum of the objective function f

$$\min_{\mathbf{x}} f(\mathbf{y}(\mathbf{x}), \mathbf{x}) \quad \text{or} \quad \max_{\mathbf{x}} f(\mathbf{y}(\mathbf{x}), \mathbf{x})$$

assuming that $y \in [\mathbf{y}_{\min}; \mathbf{y}_{\max}]$; $\mathbf{x} \in [\mathbf{x}_{\min}; \mathbf{x}_{\max}]$, where f is an objective function, \mathbf{y} – vector of assumed flow parameters; \mathbf{x} – vector of assumed geometrical parameters.

In this paper, the shape optimisation of selected turbine stages is carried out with the help of a code Optimus [12]. As objective functions in this code, the following functions can be optimised: moment of force at the rotor blades or stage power, efficiency or energy losses of the stage, both total or static. Here, the optimised (minimised) objective function is the total loss of the stator-rotor stage (with the exit kinetic energy also considered a loss). The following parameters of blade shape can be considered during the optimisation for each blade row: blade number, stagger angle, blade height, linear twist angle, linear lean angle, and linear sweep angle, 4 parameters of compound twist (2 at hub, 2 at tip), 4 parameters of compound lean (2 at hub, 2 at tip), and 4 parameters of compound sweep (2 at hub, 2 at tip). Each parameter is allowed to vary in a prescribed range of variation.

In order to secure global flow conditions, there are also constraints imposed on the mass flow rate, exit angle, average reaction, reaction at tip and root. The exit angle and reactions are not allowed to assume values beyond the prescribed ranges, which is pronounced in the form of the objective function: $f = \zeta$, if the exit angle and reactions fall within the prescribed range, or $f = \infty$, otherwise, or also if the calculations failed, where ζ is a value of an optimised characteristic obtained from the RANS solver.

The penalty function is imposed on the mass flow rate if it falls beyond the required interval $[G_-, G_+]$: $f = \zeta$, if $G_- \leq G \leq G_+$, or $f = \zeta + \min[(G - G_{\pm})^2]/\varepsilon$, otherwise, where G is the current mass flow rate, ε – penalty weight coefficient.

Method of deformed polyhedron

As it is difficult in general to make a priori assumption concerning the smoothness of the objective function, non-gradient methods of optimisation are used in the code Optimus. The method applied here is Nelder-Mead's method of deformed polyhedron [13], based on the earlier simplex method, see Spendley *et al.* [14].

An essential feature of the method of deformed polyhedron is that, unlike its prototype of the simplex method, the deformed polyhedron adapts to changing topography of the objective function, by virtue of its reflecting, stretching and compression properties. This enables us to find the extremum of the objective function even far away from the initial polyhedron. Of great importance for effective operation of the algorithm is appropriate selection of the reflection ratio α , compression ratio β , stretching ratio γ and reduction ratio δ . The recommendation of Nelder and Mead, and also the experience of the authors suggest that the following values be used $\alpha = 1$, $\beta = \delta = 0.5$ and $\gamma = 2$.

The efficiency of the method of deformed polyhedron, measured by the number of calculations of the objective function during one iteration, does not depend on the number of optimised parameters and for the majority of cases is limited to 2–3 calculations per iteration. The method usually enables efficient optimisation of 5–8 or even 10 geometrical parameters of the considered turbine/compressor stages and is relatively easy to work with constraints imposed on the mass flow rate, reaction and exit angle. However, it should be mentioned that the attempts to prove the convergence of the method for wide classes of functions have failed, Torczon [15]. Some numerical experiments also show that the method is not always convergent, especially when the number of parameters exceeds 7. Nevertheless, even in this case it can still produce solutions whose objective function is better than that of the initial design.

3. 3D RANS solver

CFD computations are performed with the help of a code FlowER – solver of viscous compressible flows through multi-stage turbomachinery developed by Yershov and Rusanov [16]. The solver draws on the set of thin-layer Reynolds-averaged Navier-Stokes equations for perfect gas. The effects of turbulence are taken into account with the help of a modified algebraic model of Baldwin-Lomax [17] without the wall function. The governing equations are solved numerically based on the Godunov-type upwind differencing and high resolution ENO scheme [18] for the calculation of

convective derivatives, assuring second-order accuracy everywhere in space and time, and third-order accuracy locally. The computational domain also extends on the radial gap above the unshrouded rotor blade tips. The following boundary conditions are incorporated: no-slip and no heat flux at the walls; span-wise distribution of the total pressure, total temperature and flow angles at the inlet to the stage; at the exit a mid-span value of the static pressure with the radial equilibrium equation assumed there. The computations carried out in one blade-to-blade passage of the stator and rotor converge to a steady state, with the condition of spatial periodicity, and a mixing plane approach assumed that makes use of a concept of pitch-wise averaging of flow parameters in the axial gap between the stator and rotor. The assumed inlet/exit boundary conditions impose the pressure drop and let the mass flow rate be resultant. An H-type multi-grid is used, with grids refined at the endwalls, blade walls and at the leading and trailing edges of the blades.

Before the available computer resources enable optimisation on refined grids, 3D computational grids used during optimisation are relatively coarse and an assumption is made that major tendencies in changing flow patterns with changing geometry of the turbine/compressor stage can already be discovered on coarse grids. The authors support this thesis, nevertheless, at least the original and final geometry must be checked on refined grids, and possible changes in flow patterns and efficiency gains must be implied based on a comparison of post-optimisation computations of the original and final geometry on refined grids.

4. Optimisation of a highly-loaded gas turbine stage (GTS)

This gas turbine stage with shrouded blades operates at a large pressure drop from 0.77 to 0.25MPa, inlet temperature 1420K, mass flow rate 1.76kg/s, rotor rotational speed 53000rpm and average reaction 40%. The stage power is 17.5kW. Initial geometrical parameters of the stator and rotor are given in Table 1. Stator and rotor stagger angles and geometrical exit angles are defined with respect to the cascade front. Both stator and rotor blades have changing cross-sections from hub to tip. Rotor blades are twisted.

Table 1. GTS – initial geometrical parameters

Parameter	Stator	Rotor
span/chord	0.44	0.87
pitch/chord	0.77	0.77
diameter/span	10.7	9.6
geometrical exit angle α_g [°]	17.3	25.3
blade number	19	34
stagger angle at hub [°]	33	60
twist angle from hub to tip [°]	0	-21

Six geometrical parameters have been chosen for optimisation:

- stator and rotor blade stagger angle,
- stator and rotor blade linear twist angle,
- stator blade linear lean and sweep angle.

Computations during the optimisation were carried out on a grid of 120 000 cells in total (stator + rotor – $2 \times 32 \times 32 \times 60$), verifying computations – on 800 000 cells ($2 \times 64 \times 64 \times 96$). The objective function was the total energy loss with the exit kinetic energy considered a loss. A penalty was imposed on the mass flow rate if it changed by more than 1%, compared to the original geometry. The average reaction was assumed not to exceed the original value. The process of optimisation has converged with the prescribed accuracy after 72 iterations (with 135 geometries calculated). Original and final values of the optimised parameters are given in Table 2.

The following tendencies have been observed:

- slightly decreasing the stator stagger angle by 0.4° with increasing the rotor stagger angle by 0.5° , meaning closing throats in the stator and opening in the rotor, which is likely to bring the reaction down, say, evenly span-wise;
- introducing a slight stator blade twist by -0.4° and more significant reduction of rotor blade twist by -1.1° , this will further open throats towards the tip in the rotor and close in the stator, bringing the reaction down towards the tip;
- leaning the stator blade tip by 3.3° with rotation of the moving blade; straight lean induces opposing effects with respect to both endwalls depending on the lean direction; in the considered case of positive lean, the reaction increases at the root, decreases at the tip, reducing the span-wise gradient of reaction; the stator blade is unloaded at the root, reloaded at the tip, with the opposite effects in the rotor [11];
- sweeping the stator blade tip by 4.2° backward; straight sweep generates opposing effects with respect to both endwalls as well as opposing effects with respect to the leading and trailing edge of the swept stator blade; in the considered case of straight sweepback, the stator blade trailing edge is unloaded at the root, reloaded at the tip [8]; this is likely to induce effects in the rotor similar as in the case of positive lean.

Table 2. GTS – original and final values of the optimised parameters

Optimised parameter	Original	Final
stator stagger angle at hub [°]	33.0	32.6
rotor stagger angle at hub [°]	60.0	60.5
stator twist angle [°]	0.0	-0.4
rotor twist angle [°]	-21.0	-19.9
stator lean angle [°]	0.0	3.3
stator sweep angle [°]	0.0	-4.2

As a result of these geometrical changes the calculated average reaction is decreased from 40% to 34%. The most spectacular changes in flow patterns are observed above the mid-span sections in the rotor where the decreased rate of acceleration on the suction surface of the rotor blade reduces the intensity of the oblique shock wave and eliminates a thick stagnation zone at the suction surface of the rotor blade downstream of the oblique shock configuration, see in Figure 1. There is also a favourable effect of reduction in transonic/supersonic velocities in the stator at the root due to the increased reaction there, and a reduction of the exit energy. Figure 2 shows the comparison of distribution of kinetic energy losses including the

exit energy. The calculated mass-averaged kinetic energy losses of the stage (with the exit kinetic energy considered a loss) are decreased by 0.7%. As the reaction is reduced at the tip there should be further gains due to reduction of tip leakage losses (not evaluated in the present optimisation).

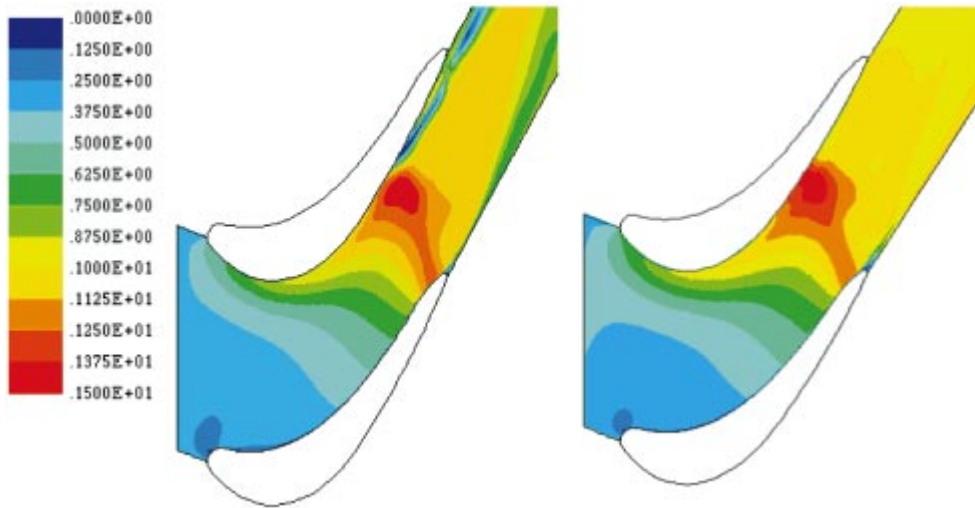


Figure 1. GTS – Mach number contours in the rotor 10% of the blade span from the tip before (left) and after (right) optimisation

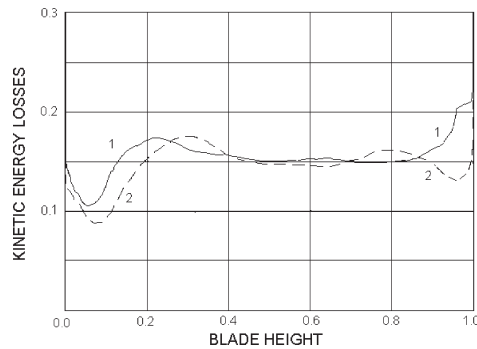


Figure 2. GTS – span-wise distribution of stage losses including the exit energy before (1) and after (2) optimisation

5. Optimisation of an HP steam turbine impulse stage (HPTS)

This HP impulse stage of a 200MW steam turbine with the originally cylindrical blades and shrouded rotor operates at a pressure drop from 0.79 to 0.71MPa, inlet temperature 760K, rotor rotational speed 3000rpm, mass flow rate 170kg/s and average reaction 19%. The stage power is 5.45MW. Initial geometrical parameters of the stator and rotor are given in Table 3.

Table 3. HPTS – initial geometrical parameter

Parameter	Stator	Rotor
span/chord	0.81	2.1
pitch/chord	0.73	0.75
diameter/span	14.4	13.6
geometrical exit angle α_g [°]	11.7	18.0
blade number	50	120
stagger angle at hub γ [°]	46	72

Nine geometrical parameters have been assumed for optimisation:

- stator and rotor blade stagger angle,
- stator and rotor blade number,
- rotor blade linear twist angle,
- stator blade compound lean displacements at the hub and tip.

Due to a large number of optimised parameters, the optimisation was carried out in two stages. In the first stage, stator and rotor blade numbers and stagger angles (4 parameters) were optimised using a 1D-based procedure [19], yielding a geometry we will refer to as intermediate. The first stage of optimisation brought a moderate change in stator and rotor blade numbers and stagger angles, see Table 4. As a result of that the calculated stage efficiency (exit kinetic energy considered a loss) increased by 0.4%. Comparative verifying computations reveal better expansion in the stator and rotor as well as a better exit angle for the same mass flow rate which reduces the exit kinetic energy.

Table 4. HPTS – original, intermediate and final values of the optimised parameter

Optimised parameter	Original	Intermediate	Final
stator blade number	50	54	54
rotor blade number	120	118	118
stator stagger angle [°]	46.0	46.8	46.9
rotor stagger angle [°]	72.0	70.5	72.6
rotor twist angle [°]	0	0	-4.1
stator compound lean displ. at hub $\Delta x/l$	0.0	0.0	-0.033
stator compound lean displ. at hub $\Delta y/l$	0.0	0.0	0.35
stator compound lean displ. at tip $\Delta x/l$	0.0	0.0	-0.073
stator compound lean displ. at tip $\Delta y/l$	0.0	0.0	0.35

Then, the intermediate geometry was subject to 3D optimisation with the rotor blade linear twist angle, stator blade compound lean displacements at hub and tip as well as stator and rotor blade stagger angles as optimised parameters (7 parameters). Note that the stator and rotor blade stagger angles should stay at the list of the optimised parameters to assure the required reaction and mass flow rate. Computations during the second stage of optimisation were carried out on a grid of 100 000 cells in total (stator + rotor – $2 \times 32 \times 28 \times 56$), verifying computations – on 800 000 cells ($2 \times 64 \times 64 \times 96$). The objective function was the kinetic energy loss including the exit energy. A penalty was imposed on the mass flow rate if it changed by more than 1%, compared to the original geometry. The average reaction was assumed not to exceed the original value. The absolute exit swirl angle was not allowed to vary

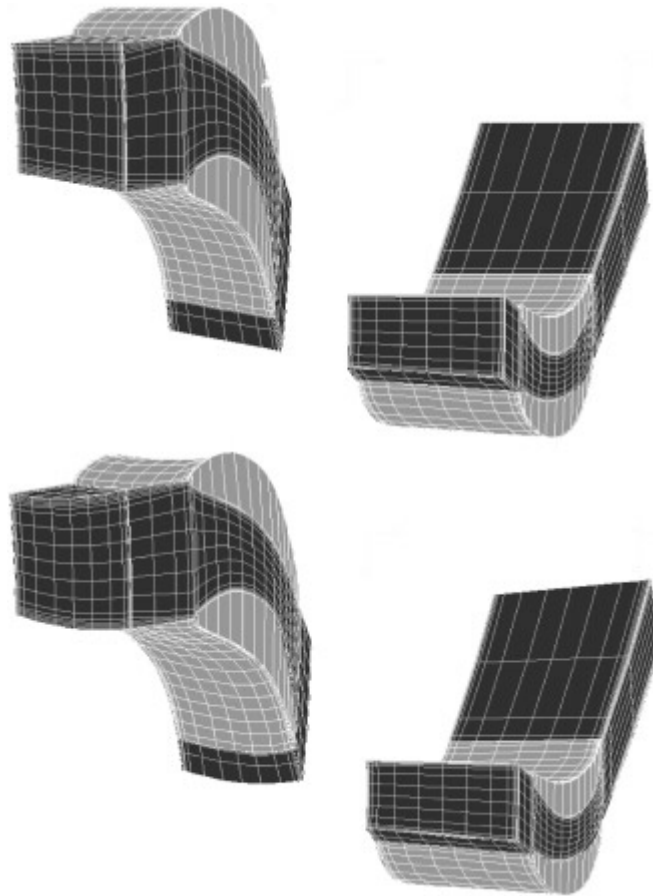


Figure 3. HPTS – a view on the computational grid (coarse grid) of stator (left) and rotor (right) of the original (top) and final (bottom) stage

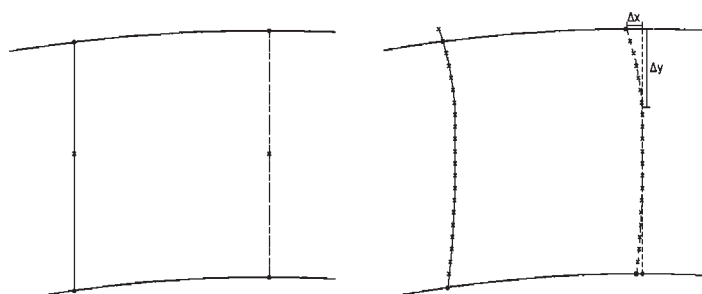


Figure 4. HPTS – original (left) and final (right) shape of stator blades in circumferential view – positive Δx refers to the direction of rotation (clockwise)

beyond the interval $(-10^\circ, 10^\circ)$. The process of optimisation has converged after 60 iterations (with 110 geometries calculated). Original, intermediate and final values of the optimised parameters are given in Table 4. Original and final geometries of flow domains, showing the shape of the blades and computational domain with a coarse grid are presented in Figure 3, whereas Figure 4 show the original and

final blades in circumferential view, explaining also the compound lean displacement parameters.

The following tendencies have been observed:

- the optimiser has chosen compound leans in the direction opposite to that of rotation at both endwalls with a larger compound lean displacement at the tip, compared to that at the hub. This direction of compound lean increases pressure at the endwalls in the stator, unloads stator blades and reduces velocities there. This should reduce the endwall losses, however, as a result of additional span-wise pressure gradient there is increased convection of boundary layer fluid to mid-span sections, which can be observed from total pressure contours downstream of the stator presented in Figure 5. As a result of changing streamwise curvature, the velocity increases at the endwalls in the rotor. More mass is passed through the endwall regions which is likely to increase endwall losses. However, the centres of loss due to secondary flows stay nearer to the endwalls, see total pressure contours downstream of the rotor in Figure 6.
- additionally, the rotor blade twist acquired during optimisation, opening throats at the hub, closing at the tip, with the increased stagger angle of the rotor blade at the hub, improves the incidence angle there. As a result, the separation zone at the front part of the rotor blade suction surface at the root is considerably reduced, which can be observed from Figure 6, and also from Figure 7 showing the entropy function contours at 8% of the blade span from the hub. The entropy function is defined here as $s = p/\rho^\gamma$, where p is the pressure, ρ – density, γ – specific heat ratio.

The presented geometrical changes brought improvements in the calculated efficiency amounting to 0.4%. Added to the previously obtained 0.4% from the blade number and stagger angle optimisation, it yields on aggregate 0.8% improvement in the calculated efficiency from the two stages of optimisation. The comparison of calculated span-wise distribution of kinetic energy losses with the exit energy in the original and final design can be seen in Figure 8. Tip leakage losses are not evaluated here.

6. Optimisation of the LP exit stage of a steam turbine (LPEX)

The optimised stage operates under a wide range of flow conditions: pressure ratio between 0.2–0.5, inlet temperature – 340–350K, mass flow rate – 35–85kg/s, exit dryness fraction $x = 0.92$ –0.98. It has diverging endwalls and twisted rotor blades. The span/diameter ratio changes between 0.25–0.35. Eight parameters were assumed for optimisation: stator straight circumferential lean, stator compound lean at root (2 parameters), stator straight axial sweep, stator compound sweep at tip (2 parameters), and stator and rotor stagger angles. The objective function was the level of kinetic energy losses in the stage, with the exit energy considered a loss. The mean exit angle was assumed not to change more than by 5° compared to the original design. The reaction at the root was assumed not to decrease below, the reaction at the tip – not to increase above that of the original design. The penalty function was

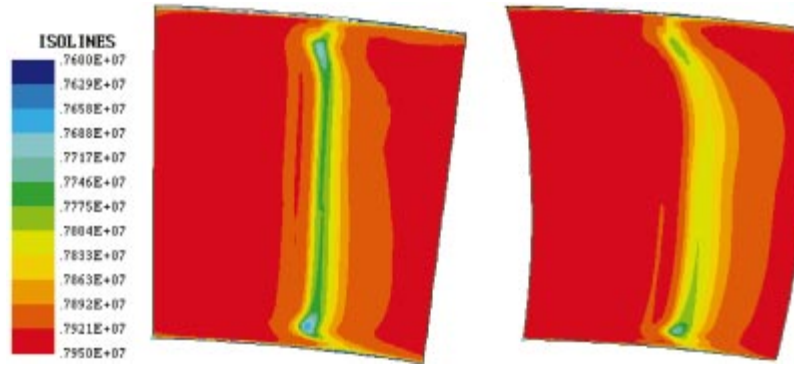


Figure 5. HPTS – total pressure contours downstream of the stator before (left) and after (right) optimisation

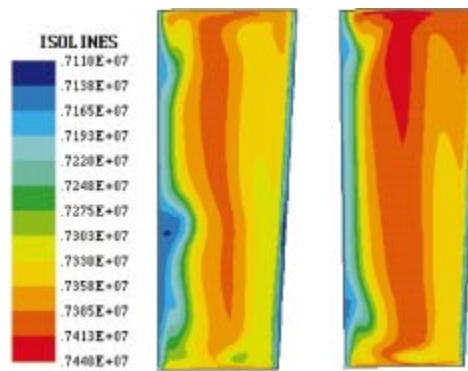


Figure 6. HPTS – total pressure contours behind the rotor before (left) and after (right) optimisation

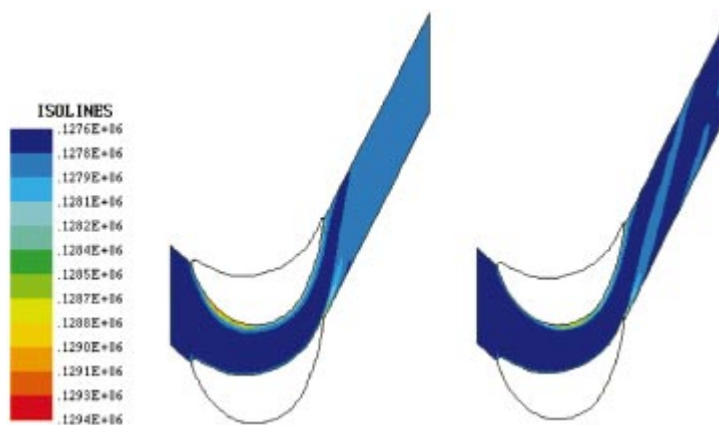


Figure 7. HPTS – entropy function contours in the rotor 8% blade span from the root before (left) and after (right) optimisation

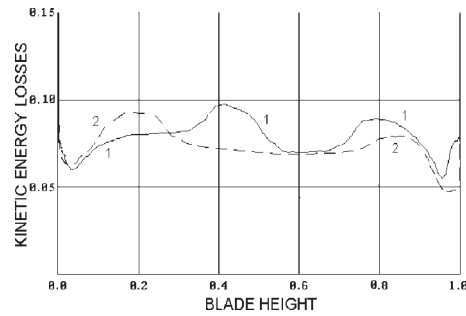


Figure 8. HPTS – span-wise distribution of kinetic energy losses including the exit energy before (1) and after (2) optimisation

imposed on the mass flow rate if it changed by more than $\pm 0.5\%$, compared to the original design.

The optimisation was carried out in the proximity of nominal operating conditions (mass flow rate – 56kg/s, pressure ratio – 0.34), however, due to the fact that exit stages of steam turbines operate over a wide range of flow rates away from the nominal conditions, the original and final geometries were also checked for low and high loads (low load mass flow rate – 38kg/s, pressure ratio – 0.51, and high load mass flow rate – 75kg/s, pressure ratio – 0.25). Due to time restrictions, RANS computations in the course of optimisation were carried out on coarse grids of 100 000 cells (stator + rotor). After optimisation, the original and optimised geometries were recalculated on more refined grids – 600 000 cells (stator + rotor). The comparative results for the reaction and losses in the original and optimised geometries presented in the paper are those of refined grids.

95 iterations were performed amounting to 180 RANS computations of different geometries. Changes in the optimised parameters of the LP exit stage are listed in Table 5. The original and final geometries are presented in Figure 9 in meridional view and circumferential view of the stator leading and trailing edges. The optimiser chose mostly axial sweeps with a considerable linear sweep (blade tip swept downstream) and compound sweep (blade tip swept upstream). The contribution of leans is not very significant, however there is some linear lean with the blade tip leaned with rotation of the rotor, and compound lean at root against rotation of the rotor. The mass flow rate remains unchanged due to corrections of the stagger angles – slightly opening throats both in the stator and rotor.

Table 5. LPEX – change of the optimised parameters

Optimised parameter	Its change
stator stagger angle increment [°]	0.5
rotor stagger angle increment [°]	0.2
stator linear sweep angle [°]	-7.4
stator compound sweep displ. at tip Δx	0.14
stator compound sweep displ. at tip Δy	0.4
stator linear lean angle [°]	-1.6
stator compound. lean displ. at hub Δx	-0.04
stator compound. lean displ. at hub Δy	0.06

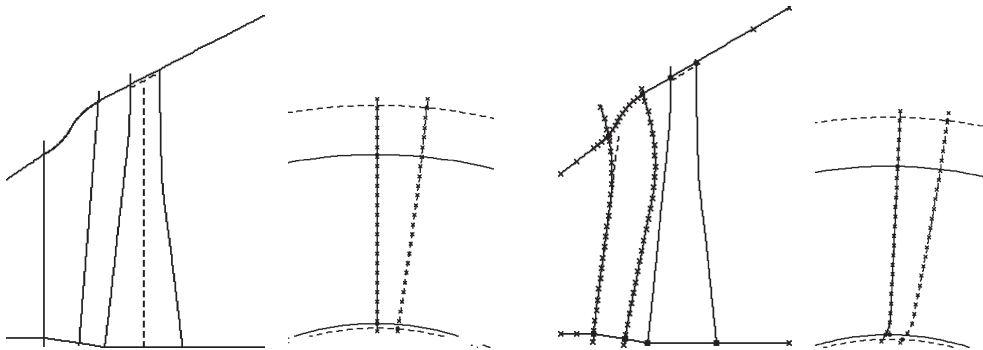


Figure 9. LPEX – original (left) and final (right) geometry in meridional and circumferential view

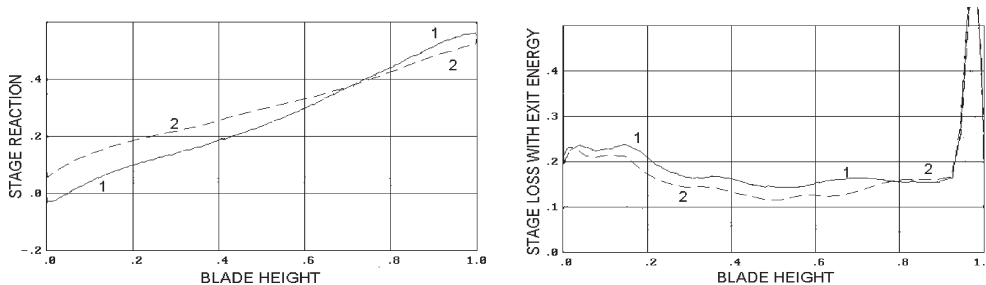


Figure 10. LPEX – span-wise distribution of reaction and stage losses before (1) and after (2) optimisation

Figure 10 shows the comparison of span-wise distribution of reaction and stage losses. There is a considerable redistribution of reaction, decreasing its span-wise gradient. The reaction is increased at the root and reduced at the tip. Transonic stator blades are unloaded at the root, reloaded at the tip, rotor blades are reloaded at the root, unloaded at the tip. There is some redistribution of the exit velocity and swirl angle. The overall stage losses with the exit energy are decreased more less evenly span-wise, on average by 1.8% for the nominal conditions. The post-optimisation computations of the design optimised for nominal conditions were made also for low load (mass flow rate – 38kg/s) giving an efficiency increase of 1.2%, and a high load (mass flow rate – 75kg/s) giving also an efficiency increase of 0.9%.

More details about authors' work on optimisation of an exit turbine stage can be found in [20] where the exit stage is optimised using, first, circumferential lean (straight and compound at the root), and then, separately, axial sweep (also straight and compound at tip). This paper shows that the efficiency gains from the application of axial sweep (optimised for the nominal load) are the highest for the nominal load and, remain moderate for low and high loads. The design with circumferential lean (also optimised for the nominal load) gives efficiency gains for the nominal load lower than the axial sweep. On the other hand, it can give much higher efficiency gains for low loads (much higher than for the nominal load for which the stage is optimised), however, producing possible efficiency losses for high loads. The conclusion of paper [20] is that the choice of either lean or sweep for the exit stage should be up

to the designer, depending on the expected time of operation within particular flow regimes.

The optimisation was carried out on coarse grids, using constraints on mass flow rate, reactions and exit swirl angle. These constraints were also held during verifying computations of the original and final geometries on refined grids. Efficiency gains obtained on refined grids did not differ by more than 0.2% from those obtained during the optimisation of the objective function on coarse grids. This is to confirm that main tendencies in changing turbine flow patterns and efficiencies due to changing geometry can already be discovered on coarse grids.

7. Conclusions

Two HP turbine stages and one LP exit turbine stage were optimised during the constrained direct efficiency-based optimisation using the combination of Nelder-Mead's method of deformed polyhedron with a 3D RANS solver. Among the optimised parameters were stator and rotor blade numbers, stagger and twist angles, stator sweep and lean, both straight and compound. The optimised stages acquired new 3D stacking lines, which gave significant improvements in their performance.

References

- [1] Demeulenaere A, Van den Braembussche R 1998 *ASME J. Turbomachinery* **120** 247
- [2] Damle S, Dang T, Stringham J and Razinsky E 1998 *ASME Paper* **98-GT-115**
- [3] Pierret S and Van den Braembussche R 1998 *ASME Paper* **98-GT-4**
- [4] Pierret S 1999 *VKI LS 1999-02 on Turbomachinery Blade Design Systems*
- [5] Shahpar S 2000 *ASME Paper* **2000-GT-523**
- [6] Lee S Y and Kim K Y 2000 *ASME Paper* **2000-GT-0488**
- [7] Harrison S 1992 *ASME J. Turbomachinery* **114** 184
- [8] Denton J D and Xu L 1999 *VKI LS 1999-02 on Turbomachinery Blade Design Systems*
- [9] Singh G, Walker P J and Haller B R 1995 *Proc. Europ. Conf. Turbomachinery Fluid Dynamics and Thermodynamics Aspects*, Erlangen, Germany
- [10] Wang Z 1999 *VKI LS 1999-02 on Turbomachinery Blade Design Systems*
- [11] Lampart P and Gardzilewicz A 1999 *Turbomachinery (Ciepłne Maszyny Przepływowe)* **115** 297
- [12] Yershov S, Shapochka A and Rusanov A 2000 *Proc. Conf. Improvements in Turbomachinery Using Methods of Mathematical and Physical Modelling*, Kharkov-Zmiev, Ukraine, pp. 171–178 (in Russian)
- [13] Nelder J A and Mead R 1965 *Computer Journal* **7** (1) 308
- [14] Spendley W, Hext G R and Himsforth F R 1962 *Technometrics* **4/441**
- [15] Torczon V J 1989 *Multi-directional search: A direct search algorithm for parallel machines* PhD Thesis, Rice University, Houston, Texas, USA
- [16] Yershov S and Rusanov A 1996 *The application package FlowER for the calculation of 3D viscous flows through multistage turbomachinery* Certificate of Ukrainian State Agency of Copyright and Related Rights, Kiev, Ukraine (in Ukrainian)
- [17] Baldwin B S and Lomax H 1978 *AIAA Paper* **78-257**
- [18] Yershov S and Rusanov A 1996 *Proc. 3rd Colloquium Process Simulation*, Espoo, Finland, pp. 69–85
- [19] Gardzilewicz A 1984 *Rep. Inst. Fluid Flow Machinery* **161/84**, Gdansk, Poland (in Polish)
- [20] Lampart P and Yershov S 2001 *ASME PVP* **424-2** 115

